

Estimation on the 3D Porosity of Plain Weft Knitted Fabric under Wale Extension

Sahar Abdolmaleki and Ali Asghar Asghariyan Jeddi

Abstract—In the recent paper [1], the Bentoufa theoretical model was improved to estimate the three dimension (3D) porosity of plain weft knitted fabric while was subjected to extension under different uniaxial extension in course direction. In addition to this model, there are only a few geometrical models for estimation of 3D porosity of weft knitted fabrics such as Bentoufa and Karaguzel models. In the present research, plain knitted fabrics over a different range of knitting stiffness are produced to investigate the accuracy of these models. Thereafter, the estimated 3D porosities of the fabrics using the theoretical models are compared with the experimental values which are obtained from Guidoin empirical model while is subjected to extension under different uniaxial extension in wale direction. It is concluded that Karaguzel and i-model models show reliable and trustful result while, Bentoufa model shows huge differences in comparison with Guidoin model.

Key words: Three dimension porosity, plain weft knitted fabric, wale extension

I. INTRODUCTION

Porosity is one of the important physical properties which are usually considered in chemical, environmental, sailing and medicine industries [2]. It is the ratio of the total amount of void space in a material to the bulk volume occupied by the material. Porosity is considered to be one of the basic features which representing a textile structure. The properties of fabric were analyzed by determining the efficiency of fabric porosity [3]. Overall, the 3D (3 volume or dimension) porosity of knitted fabrics can be evaluated through two methods:

Firstly, Experimental methods including optical techniques as well as methods on the basis of liquid penetration, absorption, filtration, and airflow that have been developed to determine the fabric's porosity [3]. Secondly, geometrical modeling which is focused on defining the loop shape and geometrical parameters.

Karaguzel [4] proposed a geometrical model to predict the pore size and pore volume for simple weft knitted structure. He obtained the following formulation to determine the porosity of plain weft knitted structure:

$$\begin{aligned} \text{Porosity}(\%) &= 100 \frac{V_{\text{void}}}{V_{\text{total}}} = 100 \frac{V_{\text{porosity}}}{V_{\text{total}}} \\ &= 100 \left(1 - \frac{sl\pi d^2}{4t} \right) \end{aligned} \quad (1)$$

where, V_{void} is void volume, V_{total} is total volume, t is fabric thickness, s is stitch density and d is the yarn diameter and l is stitch length (obtained from the Peirce's stitch length model i.e. $l=2C+W+5.94d$).

In order to determine the porosity in weft knitted fabric, Bentoufa [2] presented his structural model based on the Suh's loop model [5]. According to the assumption of Suh, yarns have a circular cross-section and uniform diameter. At the end, Bentoufa obtained a new formulation to determine the porosity of plain weft knitted structure as shown by Eq. (2).

$$\text{Porosity}(\%) = 100 \times \left(1 - \frac{\pi d^2 \left(8C + (2d + W) \sqrt{1 + \frac{d^2}{C^2}} \left(\pi - 2 \text{tg}^{-1} \left(\frac{d}{C} \right) \right) \right)}{16tW(d + C + 2y)} \right) \quad (2)$$

where, d is yarn diameter, t is fabric thickness, C is course spacing, W is wale spacing and y could be calculated from Eq. (3).

$$y = \left(\frac{W}{4} + \frac{d}{2} \right) \left[\sqrt{1 + \frac{d^2}{C^2}} - \frac{d}{C} \right] \quad (3)$$

Abdolmaleki *et al.* [1] investigated recently 3D porosity of plain knitted fabric under course extension and they did some changes on Bentoufa model to minimize the difference between the fabric porosities under uniaxial tension which was calculated based on Bentoufa model and experimental data. They identified an improved model (i-model) and finally modified the following formula:
Porosity = 100 ×

$$\left(1 - \frac{\pi d^2 \sqrt{1 + \frac{d^2}{C^2}} \left(C + \left(\frac{W}{4} + \frac{d}{2} \right) \left(\pi - 2 \text{tg}^{-1} \left(\frac{d}{C} \right) \right) \right)}{2WCt} \right) \quad (4)$$

where, C is course spacing, W shows the wale spacing, t is fabric thickness and d stands the yarn diameter.

In empirical Guidoin's study [6], porosity was defined as the ratio of void space or volume of pores within the boundaries of a solid material to the total volume. He

modified his formula as follows:

$$\begin{aligned} \text{Porosity}(\%) &= 100 \left(\frac{V_v}{V_t} \right) = 100 \left(1 - \frac{\rho_t}{\rho_m} \right) \\ &= 100 \left(1 - \frac{M}{t \cdot \rho_m} \right) \end{aligned} \quad (5)$$

where, M is weight per unit area of porous material (g/cm^2), t is thickness of porous material (cm), ρ_m is density of solid material (g/cm^3), ρ_t is overall density of porous material (g/cm^3), V_v is volume of void space (cm^3) and V_t is total volume of porous material (cm^3).

The object of the work described in this article is to consider the 3D porosity of plain weft knitted fabric while is subjected to extension under different wale extension. This investigation has been performed experimentally based on Guidoin method, then compared with the calculated values according to the 3D theoretical methods suggested by Benltoufa and Karaguzel as well as i-model.

II. EXPERIMENTAL

Plain weft knitted fabrics with three different stitch lengths ($L_1=2.2$ mm, $L_2=2.49$ mm and $L_3=3.35$ mm) were produced on a circular knitting machine with 34" diameter and 26 gauge cylinder from 164 dtex textured polyester yarn. From each fabric structure, 15 specimens of the size 18.5×7 cm^2 were cut in the wale direction. In the middle of each fabric specimen, a square of the size 4×4 cm^2 was drawn in order to neutralize the effect of curling in fabric's edge for the accuracy of the measurement. It should be noted that any considerable bow tendency of the sample fabrics during extension test was not observed. Then, each specimen was extended under ten different wale extensions from 0% to 45% at extension intervals of 5%. The fabric extension was performed using an especial extended apparatus which was designed and manufactured for this purpose, shown in Figure 1 [7].

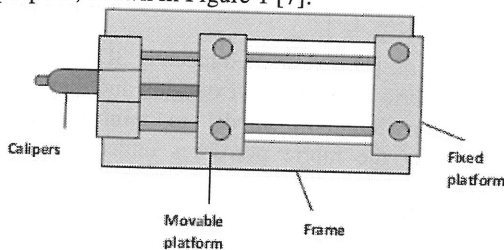


Fig. 1 The apparatus used for extended fabrics [7].

III. RESULTS AND DISCUSSIONS

A. Porosity consideration under extension in wale direction

The experimental porosities of the plain knitted fabrics were measured based on the empirical Guidoin's model, i.e. Equation (5), with assumption $\rho_m = \rho_{\text{yarn}} = 0.621$ g/cm^3 for all samples under different extension. To measure M_0 (weight per cm^2 under zero extension), the 18.5×7 cm^2 specimen was weighted. Thereafter, M_0 was calculated. As mentioned earlier, a square of 4×4 cm^2 was

drawn in every specimen. Therefore, the weight of this square area in zero extension was calculated using M_0 value. However under extensions, the square area changed to the rectangular shape but its weight remained constant. To measure the fabric specimen's thickness, the MITUTOYO-NO.7323 apparatus with 0.001 mm sensitivity was used and 20 readings were performed for each specimen and the average was considered as the thickness of the specimen in specific extension. To investigate the fabric porosities while subjected to extension in wale direction, Guidoin experimental model was also used as reference model. The weight per cm^2 (M) showed a decreasing trend at initial extensions in all the samples (Table I). Also, from Table I is evident that for the same range of extensions, thickness (t) also decreases nearly in the same trend as (M) therefore, the value M/t does not significantly vary. The statistical analysis showed that, the fabric porosities do not change significantly at initial extensions (Table II and Fig. 2). However, as the applied extension is increased, not only the thickness (t) is reduced, but also weight per cm^2 (M) increases (Table I). These changes make for a considerable increase in the ratios of weight per cm^2 to thickness (M/t) (Table I) and initiate porosity reductions. Data obtained from Guidoin method confirm these observations (Fig. 2).

TABLE I
VARIATION OF WEIGHT PER UNIT AREA (M), THICKNESS (T) AND THE (M/T) UNDER THE EXTENSION IN WALE DIRECTION

Ext. (%)	$L_3=3.35$ mm			$L_2=2.49$ mm			$L_1=2.2$ mm		
	M (g/cm ²)	t (cm)	M/t (g/cm ³)	M (g/cm ²)	t (cm)	M/t (g/cm ³)	M (g/cm ²)	t (cm)	M/t (g/cm ³)
0	0.120	0.57	2.111	0.147	0.486	2.959	0.159	0.521	3.042
5	0.117	0.56	2.099	0.146	0.493	2.972	0.156	0.511	3.053
10	0.114	0.554	2.049	0.148	0.486	3.05	0.154	0.498	3.099
15	0.111	0.542	2.04	0.151	0.474	3.192	0.154	0.485	3.167
20	0.109	0.527	2.075	0.156	0.454	3.433	0.154	0.472	3.273
25	0.109	0.508	2.152	0.161	0.433	3.706	0.158	0.458	3.416
30	0.110	0.485	2.278	0.165	0.410	4.031	0.158	0.443	3.555
35	0.113	0.464	2.440	0.170	0.390	4.380	0.160	0.430	3.712
40	0.118	0.438	2.706	0.173	0.370	4.680	0.161	0.417	3.866
45	0.124	0.411	3.047	0.175	0.356	4.967	0.165	0.405	4.064

* extension **weight per cm^2 (g/cm^2) ***thickness (cm) **** $\frac{M}{t} = \frac{\sum_{i=1}^{15} (M_i)}{t_i}$

TABLE II
RESULTS OF DUNCAN TEST ON GUIDOIN 3D POROSITY ON TENSION AT WALE DIRECTION

Loose knitted (L ₂ =3.35 mm) subset		Moderate knitted (L ₂ =2.49 mm) subset															Tight knitted (L ₂ =2.2 mm) subset	
Ext%	Porosity % (Guidoin)	Ext%	Porosity % (Guidoin)	Ext%	Porosity % (Guidoin)	Ext%	Porosity % (Guidoin)	Ext%	Porosity % (Guidoin)	Ext%	Porosity % (Guidoin)	Ext%	Porosity % (Guidoin)	Ext%	Porosity % (Guidoin)	Ext%	Porosity % (Guidoin)	
45	50.91	45	20.97	45	34.96	45	50.14	45	52.35	45	49.01	45	50.10	45	50.83	45	51.01	
40	56.42	40	24.96	40	37.73	40	50.98	40	47.28	40	48.01	40	50.10	40	50.83	40	51.01	
35	60.90	35	29.76	35	40.18	35	44.71	35	45.01	35	47.28	35	50.10	35	50.83	35	51.01	
30	63.31	30	35.06	30	42.57	30	40.37	30	45.01	30	47.28	30	50.10	30	50.83	30	51.01	
25		25	40.37	25	44.18	25	44.71	25	45.01	25	47.28	25	50.10	25	50.83	25	51.01	
20		20	44.71	20	45.01	20	45.01	20	45.01	20	47.28	20	50.10	20	50.83	20	51.01	
15		15	48.59	15	45.01	15	45.01	15	45.01	15	47.28	15	50.10	15	50.83	15	51.01	
10		10	50.98	10	45.01	10	45.01	10	45.01	10	47.28	10	50.10	10	50.83	10	51.01	
5		5	52.35	5	45.01	5	45.01	5	45.01	5	47.28	5	50.10	5	50.83	5	51.01	
0		0	52.35	0	45.01	0	45.01	0	45.01	0	47.28	0	50.10	0	50.83	0	51.01	

B. Verification of the theoretical models under extension in wale direction

In order to verify the correctness and accuracy of Benltoufa, Karaguzel and i-model models under wale extension, their results (based on the Eqs. (1), (2), and (4) respectively) were calculated. For calculating the yarn diameter, it was assumed that the yarn diameter (cm) under different extension remains constant. Then, the calculated results of the 3D porosity by theoretical models are compared in Figs. 3, 4 and 5 to those obtained experimentally. Results from Guidoin empirical model and the theoretical models indicate that porosities decrease by increasing the percentage extension. However, there is an exception at the initial extension for loose fabrics that showed a small increase only for Guidoin model. However, such small increasing had not any statistical significantly (Tables III, IV and V).

The difference of the porosity percentage between the theoretical models and the empirical Guidoin method is given in Table VI. According to data, in compared with the result of empirical Guidoin model, the percentage difference of Karaguzel and i-model models are much smaller compared to that of Benltoufa model. Hence, data from Karaguzel and i-model models can be effective tools to estimate the percentage porosities of the fabric under wale tension.

C. Discussion

As it can be seen from Table VII, for the loose fabric (L₂=2.49mm), both the fabric thickness (t) and weight per cm² (M) are decreased with increasing of extension in course direction. However, these decreasing are such that cause finally the ratios of weight per cm² to thickness (M/t) to be decreased. Hence, the fabric's porosity is increased due to increasing of extension in course direction. On the other hand, Table VII shows that, for the tight fabric

(L₁=2.2mm), up to the moderate amounts of extension (15%), the value of M/t does not vary significantly. Therefore, 3D porosity will not be changed significantly up to the moderate extensions. While, with more extension this ratio is increased which causes 3D porosity will be decreased (Table VIII).

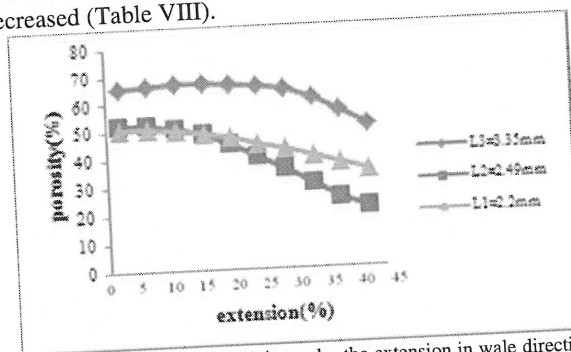


Fig. 2. Variations of fabric porosity under the extension in wale direction (Guidoin method).

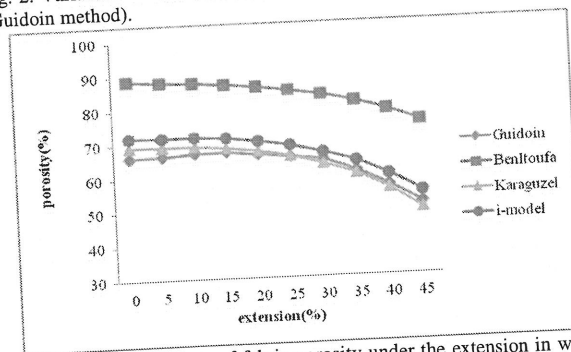


Fig. 3. Obtained variations of fabric porosity under the extension in wale direction which calculated by different models (L₂=3.35 mm).

Based on the recent paper [1], by increasing the extension in the course direction, the fabric porosities would be raised up to its apex and after that with increasing the extension, porosities would be decreased. On the other side, porosities decrease by increasing the extension in the wale direction.

RESULTS OF DUNCAN TEST ON 3D POROSITY OF FABRIC UNDER TENSION AT WALE DIRECTION USING DIFFERENT THEORETICAL METHODS ($L_3=3.35$ MM)

Bentoufa subset									i-model subset									Karaguzel subset								
Ex%	1	2	3	4	5	6	7	8	Ex%	1	2	3	4	5	6	7	8	Ex%	1	2	3	4	5	6	7	8
45	75.15								45	54.3								45	49.36							
40		78.86							40		59.55							40		55.34						
35			81.46						35			63.71						35			60.07					
30				83.41					30				68.44					30				63.15				
25					85.01				25					68.76				25					65.64			
20						86.21			20					70.20				20					67.33			
15							87.09		15						70.20	71.22		15					68.45			
10								87.72	10						71.22	71.72	71.78	10					68.91			
5									5						71.72	71.78		5					68.91			
0									0							72.03		0					69.2			

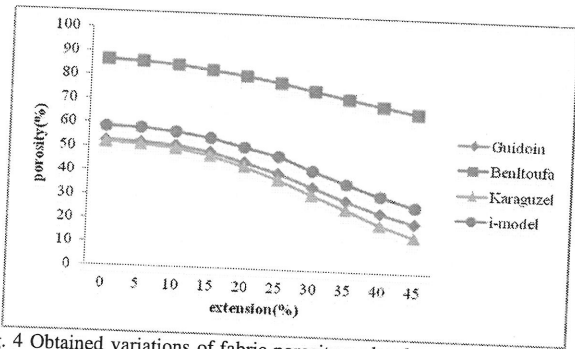


Fig. 4 Obtained variations of fabric porosity under the extension in wale direction which calculated by different models ($L_2=2.49$ mm).

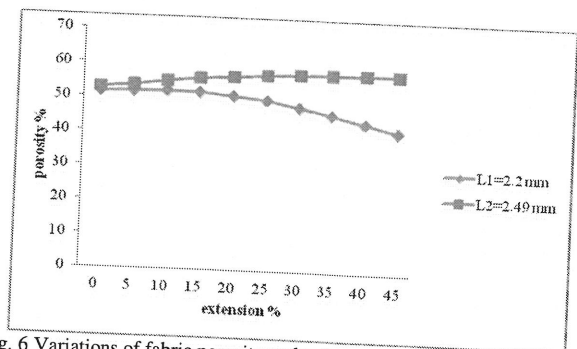


Fig. 6 Variations of fabric porosity under the extension in course direction (Guidein method) [1].

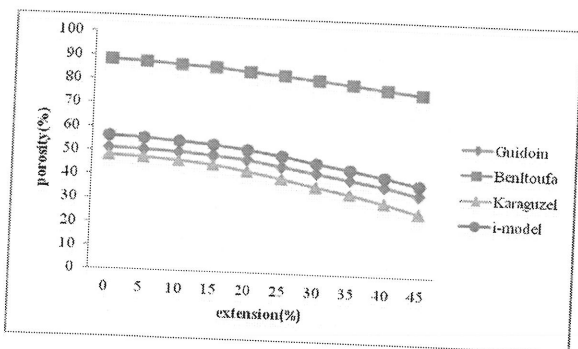


Fig. 5 Obtained variations of fabric porosity under the extension in wale direction which calculated by different models ($L_1=2.2$ mm).

To explain above trends, when fabric extends under the course direction, the load effects on its knitting cause curving of knitting would be reduced and as the result, the knitted plan would be increased so the surface porosities will be increased too. Finally, with increasing the tension at final extensions, all knitting at each wale get totally converge and cause surface porosities decrease. On the other side, by increasing the tension, the thickness of fabric would be decreased. The ratios of surface porosities to thickness has got inverse relation with 3D porosity so until the ratios of surface porosities to thickness decrease, the 3D porosity will increase and oppositely, with increasing the ratios of surface porosities to thickness, 3D porosity will decrease.

However in the wale direction, due to load effect of extension on both sides of knitted cause at initial extension, the curve of knitting will be flat and admittedly

with increasing the ratios of surface porosities to thickness, 3D porosity will be decreased.

TABLE VI
PERCENTAGE DIFFERENCE OF POROSITY BETWEEN THEORETICAL MODELS AND GUIDOIN EXPERIMENTAL METHOD AT WALE DIRECTION

Ext(%)	L ₂ =3.35 mm			L ₂ =2.49 mm			L ₁ =2.2 mm		
	Karaguzel	i-model	Benloulou	Karaguzel	i-model	Benloulou	Karaguzel	i-model	Benloulou
0	4.8	9.2	34.3	1.2	11.7	65.4	6.1	10.1	73.1
5	3.9	8.2	32.8	1.8	11.3	64.6	6.7	9.5	72.6
10	2.8	7.0	30.9	2.4	11.5	66.4	7.4	9.3	73.3
15	1.9	6.1	29.7	3.2	12.3	71	8.3	9.2	75
20	1.4	5.8	29.9	4.4	14.1	80.9	9.6	9.3	78.6
25	0.4	5.2	30.1	6.1	17.9	94.3	11	9.9	84.1
30	0.3	4.9	31.7	8.9	19.7	115	13	10.2	90.8
35	1.4	4.6	33.8	12.7	24.3	144	15.2	10.7	98.1
40	1.9	5.5	39.4	18.5	29.2	180	18.2	10.7	106
45	3.1	6.6	47.6	27.2	32.8	219	21.6	12	120

TABLE VII
VARIATIONS OF WEIGHT PER UNIT AREA (M), THICKNESS (T) AND THE RATIO (M/T) UNDER THE EXTENSION IN COURSE DIRECTION [1]

Ext(%)	L2=2.49 mm			L1=2.2 mm		
	M (g/cm ²)	t (cm)	M/t (g/cm ³)	M (g/cm ²)	t (cm)	M/t (g/cm ³)
0	.0148	.0508	.2929	.0156	.0518	.3010
5	.0142	.0496	.2874	.0151	.0505	.2990
10	.0137	.0490	.2796	.0146	.0492	.2978
15	.0132	.0482	.2739	.0143	.0478	.2995
20	.0128	.0475	.2695	.0141	.0462	.3045
25	.0125	.0468	.2662	.0139	.0445	.3114
30	.0122	.0463	.2632	.0138	.0427	.3229
35	.0120	.0458	.2615	.0138	.0411	.3348
40	.0118	.0454	.2603	.0138	.0395	.3484
45	.0118	.0453	.2600	.0138	.0381	.3626

* extension **weight per cm² (g/cm²) ***thickness (cm) **** $= \sum_{i=1}^{15} \left(\frac{M_i}{t_i} \right)$
15

IV. CONCLUSION

- Results of Guidoin method indicated that by applying extension in wale direction the porosities decrease.
- The proposed theoretical i-model showed a

good agreement with experimental results using Guidoin empirical method for the tight fabrics at higher extensions while, the Karaguzel theoretical model is more reliable for the loose fabrics at lower extensions.

TABLE VIII
THE RESULTS OF DUNCAN TEST ON GUIDOIN 3D POROSITY ON TENSION AT COURSE DIRECTION

Ext(%)	Porosity									
	Moderate knitted (L2=2.49 mm)					Tight knitted (L1=2.2 mm)				
	subset					subset				
0	1	2	3	4	5	1	2	3	4	5
5	52.84	53.75				41.61	43.94			
10		54.97					46.08			
15		55.88						48.03		
20		56.6		56.6					49.93	
25		57.14		57.14						51.02
30		57.6		57.6						51.54
35		57.88		57.88						51.78
40		58.11		58.11						51.85
45		58.13		58.13						52.06

Acknowledment

Partial financial support of Center of Excellence of New Method of Identifications in Textile (CENMIT) is acknowledged.

REFERENCES

- [1] S. Abdolmaleki, A. A.A. Jeddi and M. Amani Tehran, "Estimation on the 3D porosity of plain knitted fabric under uniaxial extension", Journal of Fibers and polymers, Vol. 13, pp. 535-541, 2012.
- [2] S. Benltoufa, F. Fayala, M. Cheikhrouhou, and S. Ben Nasrallah, "Porosity determination of jersey structure", Autex Res J, Vol. 7, pp. 63, 2007.
- [3] E. A. Elnashar, "Volume porosity and permeability in double-layer woven fabrics", Autex Res J, Vol. 5, pp. 207, 2005.
- [4] B. Karaguzel, "Characterization and role of porosity in knitted fabrics", M.Sc. Dissertation, NCSU, USA, 2004.
- [5] M. W. Suh, "Study of the Shrinkage of Plain Knitted Cotton Fabric, Based on the Structural Changes of the Loop Geometry due to Yarn Swelling and Deswelling", Text Res J, Vol. 37, pp. 417, 1967.
- [6] R. Guidoin, M. King, D. Marceau and A. Cardou, "Textile arterial prostheses: Is water permeability equivalent to porosity?", Journal of Biomedical Material Research, Vol. 21, pp. 65, 1987.
- [7] S. A. Mirshahvalad, "Investigation inter structure of fabrics under uniaxial extension", M.Sc. thesis, Amirkabir University of Technology, Iran, 2007.

Influence of Solvent/Polymer Interaction on Miscibility of PMMA/PCL Blend: Thermal Analysis Approach

Hossein Fashandi and Mohammad Karimi

Abstract—The aim of the present work is to probe the influence of solvent on miscibility behavior of a blend of poly(ϵ -caprolactone) (PCL)/Poly (methyl methacrylate) (PMMA). PMMA/PCL blend with mass ratio of 50:50 is employed to prepare the solutions of three different solvents including tetrahydrofuran, toluene and dichloromethane. At the equilibrium situation, the separated phases are cast by film multi-applicator for solvent evaporation and analyzed using thermal analysis (DSC and DMA) approaches. According to the results, the solvent is able to change the saturation value of PCL into the PMMA-rich phase by changing the free energy of the mixture. Through the PCL melting enthalpy as well as the glass transition of PMMA, the capability of PMMA-rich phase for dissolving the PCL and vice versa is investigated. To realize the influence of solvent for these variations, Hansen solubility parameter of components is considered to analyze. It is shown that glass transition of PMMA can be reduced to low values of about 50 °C as a result of solvent-induced miscibility with PCL at room temperature which is not easily achievable by other processes.

Key words: Poly (methyl methacrylate), poly(ϵ -caprolactone), solvent-induced miscibility, thermal analysis

I. INTRODUCTION

The blend of two or more polymers is of huge interest because of economical motivations and its prominent role in developing new materials with specific characteristics [1]. On the other hand, a literature review reveals that polymer blend is the subject of a large amounts of papers published every year [2-5]. The final properties of a polymeric blend are determined by the characteristics of its components and composition, the initial mass ratio and the degree of miscibility of the components [5]. The later factor, i.e. degree of miscibility, is of prominent importance and it is essential to investigate the phase behavior of mixture by means of thermodynamics and rheology [1]. Using a common solvent to dissolve the two polymers and then drying them is a well-known practice to produce polymer alloys and blends. Thermodynamics is the key to describe the mixing behavior of the polymer blends. Generally, combinatorial entropy of mixing can be considered to be negligible when the components are macromolecules. So a negative enthalpy of mixing is needed to induce miscibility. This can be achieved by

strong specific interactions between components of the blend [6]. In the absence of such interactions, the miscibility depends on temperature, composition [6], and additives such as compatibilizers [1] and particles [7], as well as solvent [8].

Making the polymer/polymer blends at the solution state, so-called solution blending, the interaction of solvent with polymers plays an important role in tailoring the properties of polymer blends. Bank *et al.* [9] demonstrated that the compatibility of polystyrene and poly(vinyl methyl ether) varies as a function of casting solvent. They showed that, the miscibility behavior of these polymers is influenced by the solvent to such an extent that clear films is obtained by casting solutions prepared by toluene or benzene but trichloroethylene and chloroform cause these polymers to suffer from incompatibility. After Bank *et al.*, Zeman and Patterson [10] considered the impression of solvent interaction with polymers on their incompatibility. They proved that incompatibility of two polymers in solution state not only arises from unfavorable interactions between segments of two polymers but also is significantly affected by solvent interaction with individual polymers. On the other hand, even for two miscible polymers, a small difference in polymer-solvent interaction varies the compatibility behavior to a great extent which can be more impressive at low polymer concentrations.

Dubey *et al.* [11] investigated the effect of solvent on the miscibility behavior of polychloroprene-co-ethylene-propene diene terpolymer blends. They found that, applying suitable solvent would enhance the miscibility of two polymers by introducing some positive interactions between two components. The impact of solvent on the viscosity behavior of PCL/PVC (poly(ϵ -caprolactone)/poly(vinyl chloride)) blend was explored by Pingping *et al.* [12]. They verified the great influence of solvent upon the viscosity behavior of this blend and considered this strong effect as the reflection of the competition among all kinds of interactions in solution. Miscibility of poly(methyl methacrylate)/poly(vinyl acetate) in a variety of solvents was argued by Crispim *et al.* [13, 14]. They showed that the miscibility of this blend depends on the solvent used to prepare the solution; so that chloroform leads to miscibility of this blend at 30 °C and 50 °C while the blend is immiscible in dimethyl formamide at the same temperature.

PMMA/PCL blends are of medical and commercial interest because of their potential for biomedical applications and/or environmentally friendly features that

H. Fashandi and M. Karimi are with the Department of Textile Engineering of Amirkabir University of Technology, Tehran, Iran. Correspondence should be addressed to M. Karimi (e-mail: mkarimi@aut.ac.ir).